LIST OF PUBLICATIONS

1. A study of the thermal decomposition of cobalt (II) and nickel (II) oxalate dihydrate using direct current electrical conductivity measurements
   A.K. Nikumbh, A.E. Athare and V.B. Raut
   Thermochim. Acta, 186 (1991) 217-233.
2. Thermal and electrical properties of manganese (II) oxalate dihydrate and cadmium (II) oxalate monohydrate
   A.K. Nikumbh and A.E. Athare
   Thermochim. Acta, (1997) communicated
3. Direct current electrical conductivity study of the thermal decomposition of copper (II) oxalate monohydrate and zinc (II) oxalate dihydrate.
   A.K. Nikumbh and A.E. Athare
   Thermochim. Acta, (1998) communicated

Symposia

4. A study of the thermal decomposition of cobalt (II) and nickel (II) oxalate dihydrate using direct current electrical conductivity measurements
   A.E. Athare and A.K. Nikumbh
   Prox. X Indian counc. chem., Goa (1991) IO-58, Page 24.

5. A study of the thermal decomposition of copper (II) oxalate monohydrate and zinc (II) oxalate dihydrate using D.C. electrical conductivity measurements
   A.E. Athare, M.M. Raste and A.K. Nikumbh
   Proc. XI Indian counc. chem., Muzaffarpur (1992) IP-4, Page 29.
6. A study of thermal decomposition of Co(II) and Ni(II) tartarate hydrate using D.C. electrical conductivity measurements
   S.B. Mane, A.E. Athare and A.K. Nikumbh
   Proc. XII Indian counc. chem., Warangal (1993) IO-83, Page 33.
7. Electrical, magnetic and Mössbauer spectra of nickel and terbium doped γ-Fe_2O_3
   M.G. Chaskar, A.E. Athare and A.K. Nikumbh
   Proc. XIII Indian counc. chem. Jammu (1994) IO-44, Page 17.
8. Electrothermal analysis of some transition metal (II) maleates - Part I
   S.K. Pardeshi, A.E. Athare and A.K. Nikumbh
   Proc. XIV Indian counc. chem., Bombay (1995) AO-31, Page 14.
9. Use of D.C. electrical conductivity as an supplementary technique in thermal analysis of Mn(II) and Cd(II) malonates
   S.K. Pardeshi, A.E. Athare and A.K. Nikumbh
   Prov.XVI Indian counc.chem., Mangalore (1997) IP-16,Page 88.

Thermochimica Acta, 186 (1991) 217–233
Elsevier Science Publishers B.V., Amsterdam

A study of the thermal decomposition of cobalt(II) and nickel(II) oxalate dihydrate using direct current electrical conductivity measurements

A.K. Nikumbh[1], A.E. Athare and V.B. Raut

Department of Chemistry, University of Poona, Ganeshkhind, Pune 411 007 (India)

(Received 21 December 1990)

Abstract

The feasibility of using direct current electrical conductivity measurements to study the solid state reactions involved in the preparation of cobalt oxide and nickel oxide from cobalt(II) and nickel(II) oxalate dihydrate have been analysed. Investigations were carried out using atmospheres of static air, dynamic air and dry nitrogen.

The study of the isothermal decomposition of cobalt(II) and nickel(II) oxalate dihydrate at different temperatures in these three atmospheres revealed that the anhydrous complexes are formed first. In static air and dynamic air atmospheres, the cobalt oxalate then undergoes oxidation decomposition to Co_3O_4 with the probable intermediate formation of CoO along with the anhydrous complex. In dry nitrogen also, the formation of CoO is well characterized.

For nickel(II) oxalate dihydrate, the final decomposition product in all three atmospheres was found to be NiO. The conductivity measurements were supplemented with data obtained by chemical, thermal (TGA and DTA), IR spectroscopic and X-ray powder diffraction analyses. The gaseous decomposition products were characterized by gas–liquid chromatography.

INTRODUCTION

In a study of the influence of atmosphere on the thermal decomposition of hydrated iron(II) dicarboxylates, it was shown [1] that the temperature and the mechanism of decomposition of the anhydrous dicarboxylates was altered by the presence of different atmospheres. Although there have been several investigations [2–6] of the thermal decomposition of manganese, cobalt and nickel oxalates, most of these were carried out by thermogravimetric analysis in a normal atmosphere. Only two of the studies were on the same material. Wiedeman and Nehring [7] reported values of 330 and 370 °C for the commencement of decomposition of nickel oxalate in air and nitrogen, respectively; these are not in good agreement with the value of 290 °C for both atmospheres given by Doremieux and Boulle [8], who also determined the decomposition characteristics of manganese, iron, cobalt,

[1] Author to whom correspondence should be addressed.

0040-6031/91/$03.50

zinc and copper oxalate in the two atmospheres and reported a shift to lower temperatures when oxygen is present for iron, manganese and cobalt oxalates, but not for zinc and copper oxalates.

Differential thermal analysis (DTA) of these oxalates has been carried out by Ugai [9] in an unspecified but probably inert atmosphere, which yielded endothermic decomposition peaks commencing at 384 °C for manganese oxalate and 400 °C for nickel oxalate. DTA was also used by Amiel and Paulmier [10] who found the decomposition of cobalt oxalate to be endothermic in nitrogen and exothermic in hydrogen. The influence of the atmosphere on the decomposition of cobalt oxalate dihydrate was also noted by Garn and Kessler [11] in their experiments with a cylinder and piston type of sample holder designed to retain the self-generated atmospheres in TGA studies. Decomposition commenced at 250 °C when the piston was omitted as compared with 370 °C when the evolved gases were retained by the piston.

Interest has recently been shown in the use of electrical conductivity techniques in the study of solid state decomposition reactions [12–16]. The present work is concerned with the feasibility of using d.c. electrical conductivity measurements as a probe to study the progress of the thermal decomposition of cobalt(II) and nickel(II) oxalate dihydrate. The conductivity measurements were supplemented with data obtained by TGA and DTA, X-ray diffraction, IR spectroscopy and gas–liquid chromatography.

EXPERIMENTAL

Sample preparation

Cobalt(II) and nickel(II) oxalate dihydrate were prepared according to the usual procedure [17]. A mixture of 14 g of $CoSO_4 \cdot 6H_2O$ or $NiSO_4 \cdot 6H_2O$, 8 g of $Na_2C_2O_4$ and 0.25 g of $H_2C_2O_4 \cdot 2H_2O$ was placed in a three-necked flask under a stream of dry nitrogen. Oxygen-free water (150 ml) was then added, and the mixture was stirred vigorously with a magnetic stirrer. After some time, cobalt(II) oxalate dihydrate, $CoC_2O_4 \cdot 2H_2O$, or nickel(II) oxalate dihydrate, $NiC_2O_4 \cdot 2H_2O$, separated out as a fine crystalline precipitate. This was filtered, washed with cold water and dried in vacuo.

Elemental analyses were made in wt.% for $CoC_2O_4 \cdot 2H_2O$ (C, 13.0 (13.1); H, 2.06 (2.10); Co, 31.6 (32.2)) and for $NiC_2O_4 \cdot 2H_2O$ (C, 12.8 (13.1); H, 2.3 (2.2); Ni, 31.5 (32.1)) where the values in parentheses are calculated ones. The IR spectra showed frequencies corresponding to the oxalate group, hydroxyl group, metal oxygen etc. The bidentate linkage of the oxalate group with the metal was confirmed on the basis of the difference between the antisymmetric and symmetric stretching frequencies. The X-ray diffraction pattern showed that the sample was polycrystalline in nature. The presence of two molecules of water of crystallization was confirmed on the basis of the thermal analysis curves and d.c. electrical conductivity measure-

ments. The compounds $CoC_2O_4 \cdot 2H_2O$ and $NiC_2O_4 \cdot 2H_2O$ have a magnetic moment of 3.59 B.M. and 2.41 B.M. respectively, which indicates that the compounds have free spin with sp^3d^2 hybridization. For the study of the decomposition of the oxalate in dynamic air, an air compressor was used to maintain an air flow of between 80 and 85 ml min^{-1}.

X-ray diffraction analysis

The products of the decomposition of $CoC_2O_4 \cdot 2H_2O$ and $NiC_2O_4 \cdot 2H_2O$ were analysed by X-ray powder diffraction techniques, using Cu $K\alpha$ radiation (wavelength, $\lambda = 0.709$ Å; nickel filter) and a PW 1730 Philips X-ray diffractometer. The experimentally observed d spacing values and relative intensities of $CoC_2O_4 \cdot 2H_2O$ and $NiC_2O_4 \cdot 2H_2O$ were compared with those reported in the ASTM file [18,19].

Thermal analysis

Thermal analysis curves were recorded using a Netzsch instrument, for atmospheres of static air, dynamic dry nitrogen and dynamic air. The flow rate for the dynamic dry nitrogen and dynamic air was 90 ml min^{-1}. The heating rate was 3 °C min^{-1} for static air and 5 °C min^{-1} for the runs with dynamic air and dynamic dry nitrogen.

D.c. electrical conductivity measurements

The d.c. electrical conductivity was measured using a Philips PP 9004 microvoltmeter [12]. The conductivity cell was designed so that different atmospheres could be used. For the decomposition study, the heating rate was adjusted to 3 °C min^{-1}. Precautions were taken to maintain a constant rate of heating. The results, presented in terms of log σ vs $10^3 T^{-1}$ (in K^{-1}), are given in Figs. 1–3 below. The data were obtained using four different pellets of the same sample, and the pattern of the σ vs. T^{-1} plots was found to be reproducible to within ± 1 °C.

The evolution of various gases during the thermal decomposition of $CoC_2O_4 \cdot 2H_2O$ or $NiC_2O_4 \cdot 2H_2O$ was recorded using Shimadzu RIA and Hewlett-Packard instruments, with nitrogen as the carrier gas.

RESULTS AND DISCUSSION

Static air atmosphere

$CoC_2O_4 \cdot 2H_2O$

The TGA and DTA curves for $CoC_2O_4 \cdot 2H_2O$ are shown in Fig. 1(a). The dehydration of $CoC_2O_4 \cdot 2H_2O$ was indicated by the presence of an endo-

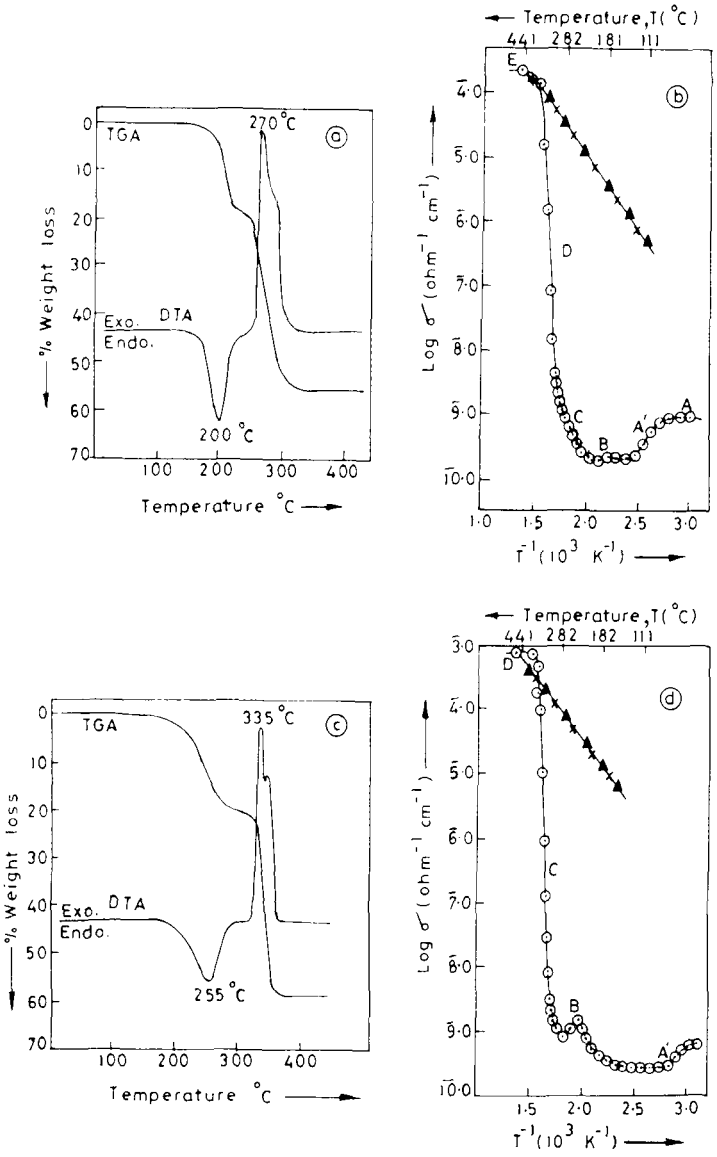

Fig. 1. Thermal decomposition in a static air atmosphere. (a) TGA and DTA curves for $CoC_2O_4 \cdot 2H_2O$. (b) Plot of log σ vs. T^{-1} for $CoC_2O_4 \cdot 2H_2O$: ○, during decomposition; ×, cooling cycle; ▲, heating cycle. (c) TGA and DTA curves for $NiC_2O_4 \cdot 2H_2O$. (d) Plot of log σ vs. T^{-1} for $NiC_2O_4 \cdot 2H_2O$: ⊙, during decomposition; ×, cooling cycle; ▲, heating cycle.

thermic peak in the DTA curves at 200 °C. The TGA curve showed a weight loss within the range 150–240 °C, with a plateau up to 255 °C, corresponding to the loss of two water molecules (calc. 19.68%; found, 20.0%). There was a sharp exothermic peak (at 270 °C) between 260 and 355 °C in the DTA curve, corresponding to the oxidative decomposition of CoC_2O_4 to Co_3O_4. The TGA curve showed a continuous weight loss within the tempera-

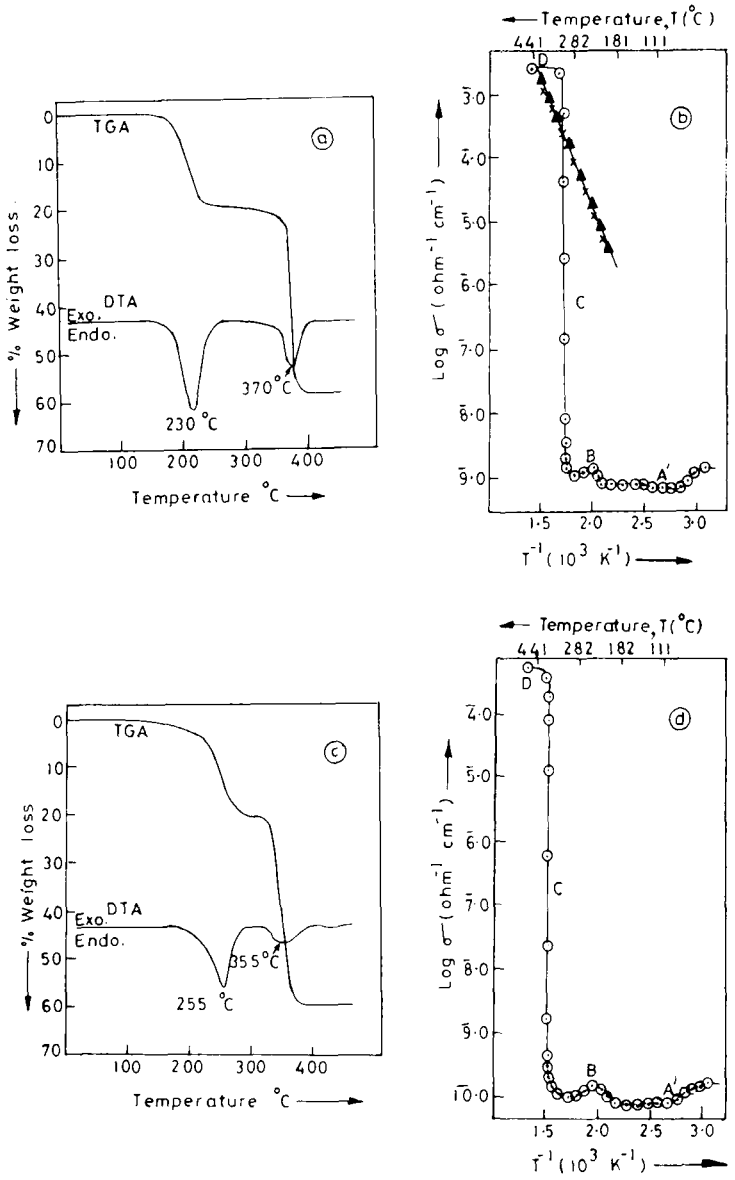

Fig. 2. Thermal decomposition in a dynamic nitrogen atmosphere. (a) TGA and DTA curves for $CoC_2O_4 \cdot 2H_2O$. (b) Plot of log σ vs. T^{-1} for $CoC_2O_4 \cdot 2H_2O$: ○, during decomposition; ×, cooling cycle; ▲, heating cycle. (c) TGA and DTA curves for $NiC_2O_4 \cdot 2H_2O$. (d) Plot of log σ vs. T^{-1} for $NiC_2O_4 \cdot 2H_2O$.

ture range 255–360 °C, corresponding to the formation of Co_3O_4 (calc., 45.37%; found, 45.05%) as final product.

A comparison of the results of conventional thermal analysis with those of conductivity analysis reveals that conductivity analysis gives a much more detailed view of the decomposition process. The temperature variation of the

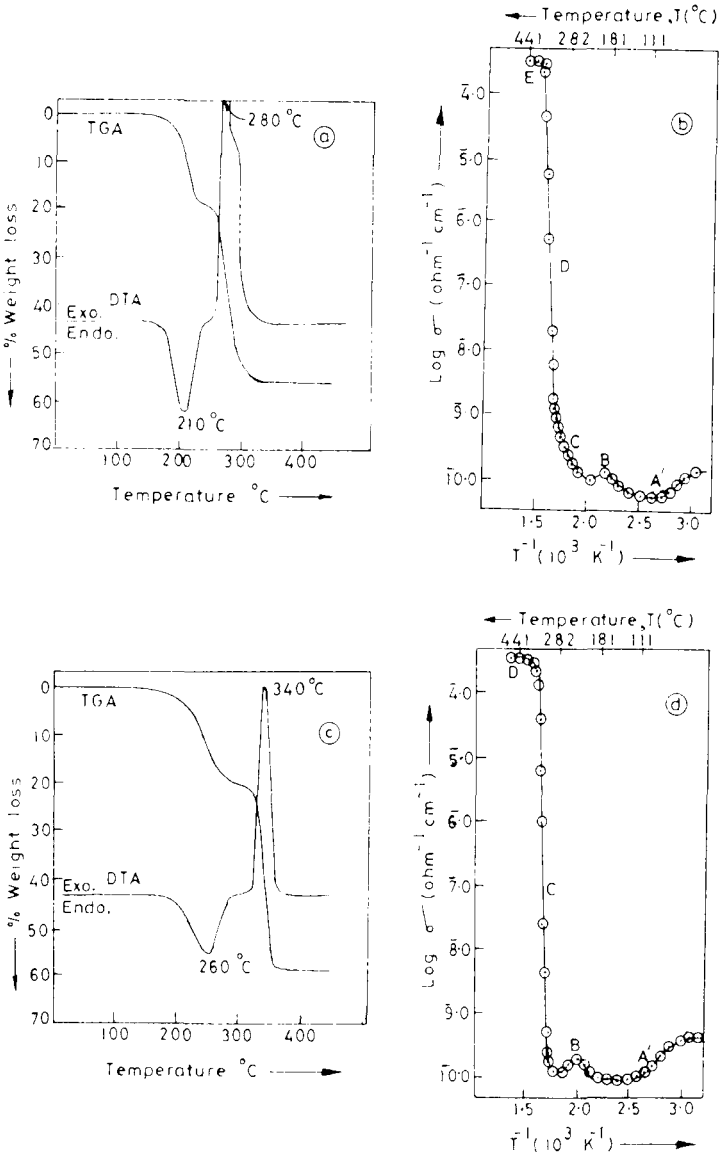

Fig. 3. Thermal decomposition in a dynamic air atmosphere: (a) TGA and DTA curves for $CoC_2O_4 \cdot 2H_2O$; (b) plot of log σ vs. T^{-1} for $CoC_2O_4 \cdot 2H_2O$; (c) TGA and DTA curves for $NiC_2O_4 \cdot 2H_2O$; (d) plot of log σ vs. T^{-1} for $NiC_2O_4 \cdot 2H_2O$.

electrical conductivity σ (Fig. 1(b)) did not show much change with an increase in temperature from 27 to 100 °C (region A). There was a steady decrease in σ between 100 and 145 °C (region A′) and the value then remained nearly constant up to 235 °C (region B). There was a steady increase in σ between 235 and 290 °C (region C), followed by a steep increase at 300 °C to a maximum at 360 °C (region D). The σ value then

increased steadily and remained almost constant in the temperature range 370–400 °C (region E).

The plot of log σ vs. T^{-1} indicated that the decomposition of $CoC_2O_4 \cdot 2H_2O$ proceeds via the formation of intermediates of varying conductivity, whereas the TGA curve obtained by conventional thermal analysis showed only a continuous weight loss, and the DTA curve showed only one sharp exothermic peak, corresponding to oxidative decomposition.

Within region A of Fig. 1(b) there was no observable change in the X-ray diffraction patterns [18] or in the IR spectra for the isothermally heated samples. The IR bands characteristic of the coordinated oxalate group [20,21] at 1600 (s) (this band was broad owing to overlap with the H_2O band), 1350 (m), 1210 (m), 815 (s) and 488 (m) cm^{-1}, persisted for samples heated up to 110 °C. In addition, bands due to coordinated water molecules were observed at 3340 (s), 1640 (s), 725 (m), 580 (m) and 535 (m) cm^{-1}. The C and H analyses were in good agreement with the formula $CoC_2O_4 \cdot 2H_2O$.

In the temperature range corresponding to region A′ in Fig. 1(b), the IR spectrum showed sharp peaks for the oxalate group frequencies, and the H–OH band decreased in intensity. The X-ray diffraction pattern also showed broad peaks with no observable change. This indicates the desorption of physically adsorbed water molecules on the upper surface of the particle surfaces [22]. A sample heated isothermally at 220 °C, in region B of Fig. 1(b), showed no H–OH bands in the IR spectrum; however, the X-ray diffraction pattern indicated a less crystalline sample, with a slight decrease in the interplanar spacings (Table 1). The elemental analysis also agreed well

TABLE 1

X-ray diffraction data for anhydrous CoC_2O_4 and NiC_2O_4 obtained from $CoC_2O_4 \cdot 2H_2O$ and $NiC_2O_4 \cdot 2H_2O$ by heating in an atmosphere of nitrogen at 250 °C and 270 °C respectively [a]

Observed d spacing for CoC_2O_4 (Å)	Observed d spacing for NiC_2O_4 (Å)
4.72 (60)	4.70 (55)
4.51 (100)	4.40 (100)
3.74 (48)	3.72 (42)
3.30 (25)	3.23 (20)
2.85 (70)	
2.70 (48)	2.78 (15)
2.39 (15)	
2.34 (30)	2.35 (50)
2.17 (21)	2.08 (22)
1.80 (10)	1.76 (30)
1.52 (18)	1.47 (10)

[a] The figures given in parentheses are intensities relative to the linewidth intensity (100).

TABLE 2

X-ray diffraction data for CoC_2O_4 and CoO obtained from $CoC_2O_4 \cdot 2H_2O$ by heating in an atmosphere of static air at 270 °C [a]

Observed *d* spacing (Å)	CoO *d* spacing [b] (Å)
4.62 (54)	
3.72 (25)	
3.26 (18)	
2.83 (45)	
2.68 (31)	
2.48 (60)	2.46 (75)
2.32 (5)	
2.15 (100)	2.13 (100)
1.80 (5)	
1.52 (40)	1.50 (50)
1.28 (23)	1.28 (20)
1.20 (15)	1.23 (16)
	1.06 (10)
0.97 (10)	0.98 (14)
0.94 (35)	0.95 (30)

[a] The figures given in parentheses are intensities relative to the linewidth intensity (100).
[b] Ref. 23.

with the anhydrous oxalate (CoC_2O_4) formulation. Region B corresponded to the dehydration of $CoC_2O_4 \cdot 2H_2O$ [2].

After the dehydration step, the value of σ increased steadily from 235 to 290 °C (region C). The IR spectrum of a sample of $CoC_2O_4 \cdot 2H_2O$ heated isothermally at 270 °C showed a decrease in the intensity of the coordinated oxalate band. Bands also appeared in the range 625–495 cm^{-1} for metal–oxygen stretching frequencies which were due to the presence of cobalt oxide [20,21]. The sample heated in this region contains 18 wt.% oxalate group (anhydrous CoC_2O_4 contains 59.89 wt.% oxalate) which indicates that this compound is possibly a mixture of CoC_2O_4 and CoO. The X-ray diffraction pattern of this isothermally heated sample (Table 2) showed generally sharp lines, indicating that the sample was predominantly crystalline. The pattern corresponded to anhydrous CoC_2O_4 and CoO [23].

A sharp increase in the value of σ was observed within the temperature range 290–360 °C (region D, Fig. 1(b)). For the sample heated isothermally at 330 °C, the IR spectrum showed a weak band corresponding to the oxalate group, but a strong, broad band was observed at 500 cm^{-1}. This band may be tentatively assigned to the Co–O stretching mode in cobalt oxide [18,19]. The X-ray diffraction pattern of this isothermally heated sample shows a complex pattern, probably that of a mixture of CoO, CoC_2O_4 and Co_3O_4. Thus the steep increase in conductivity observed in Region D was due to the transformation of CoC_2O_4 to Co_3O_4, possibly via

TABLE 3

X-ray diffraction data for Co_3O_4 obtained from $CoC_2O_4 \cdot 2H_2O$ by heating in an atmosphere of static air at 380 °C [a]

Observed *d* spacing (Å)	Co_3O_4 *d* spacing [b] (Å)
4.65 (25)	4.67 (20)
3.71 (5)	
2.86 (47)	2.86 (40)
2.44 (100)	2.44 (100)
2.32 (15)	2.33 (12)
2.02 (20)	2.02 (25)
1.83 (10)	
1.65 (8)	1.65 (12)
1.53 (40)	1.55 (35)
1.40 (48)	1.42 (45)
1.21 (10)	1.23 (12)
1.08 (7)	1.08 (8)
1.05 (12)	1.05 (16)
1.01 (12)	1.01 (16)
0.93 (18)	0.93 (15)

[a] The figures given in parentheses are intensities relative to the linewidth intensity (100).
[b] Ref. 26.

the semiconducting CoO (about $10^{-6}\ \Omega^{-1}\ cm^{-1}$) [24,25]. In this experiment, a separate step for the formation of CoO could not be identified. It should be noted here that the conductivity measurements were made on a dynamic system, while the other data were from samples obtained by isothermal heating at a specified temperature.

Within the temperature range of region E in Fig. 1b, the value of σ remained almost constant. The sample obtained by heating isothermally in static air at 380 °C showed a black oxide. The X-ray diffraction pattern observed for this region indicated a predominance of Co_3O_4 (Table 3) [26]. No line which could be assigned to metallic cobalt was detected in our work. The Co_3O_4 has an normal spinel structure and an electrical conductivity value of about $10^{-4}\ \Omega^{-1}\ cm^{-1}$ [27]. The sample thus obtained at 380 °C shows a change in σ as the temperature is changed (see cooling and heating cycle, Fig. 1(b)). This behaviour is characteristic of Co_3O_4 [27].

$NiC_2O_4 \cdot 2H_2O$

The dehydration step of nickel oxalate dihydrate, $NiC_2O_4 \cdot 2H_2O$ (see Fig. 1(c)) can be detected on the DTA curve by the single endothermic peak at 175–285 °C. The TGA curves show a weight loss for the dehydration step up to 280 °C corresponding to the loss of two water molecules. This dehydration step was also clearly indicated by the presence of a peak in region B of the log σ vs. T^{-1} plot in Fig. 1(d). The IR spectrum showed no

TABLE 4

X-ray diffraction data for NiC_2O_4 and NiO obtained from $NiC_2O_4 \cdot 2H_2O$ by heating in an atmosphere of static air at 350 °C [a]

Observed *d* spacing (Å)	NiO *d* spacing [b] (Å)
4.68 (15)	
4.38 (35)	
3.90 (5)	
3.72 (10)	
2.78 (5)	
2.41 (60)	2.41 (60)
2.10 (100)	2.09 (100)
1.74 (18)	
1.50 (35)	1.47 (35)
1.26 (25)	1.26 (18)
1.20 (20)	1.20 (16)
1.05 (10)	1.04 (8)
0.97 (8)	0.96 (6)
0.88 (8)	0.85 (10)
	0.80 (5)

[a] The figures given in parentheses are intensities relative to the linewidth intensity (100).
[b] Ref. 28.

H–OH band for $NiC_2O_4 \cdot 2H_2O$ heated isothermally at 250 °C. X-ray diffraction (Table 1) and elemental analysis corresponded to the formula NiC_2O_4 [2].

The oxidative decomposition of $NiC_2O_4 \cdot 2H_2O$ was indicated by the very strong broad exothermic peak on the DTA curve at 310–370 °C. The TGA curve showed a continuous weight loss from 310 °C until the sample crystallized to mainly NiO. The plot of log σ against T^{-1} showed a steep increase in σ at 300–365 °C (region C) and then remained constant above this temperature (region D). The X-ray diffraction pattern of this isothermally heated sample (region C) showed a generally sharp line, indicating that the sample was predominantly crystalline. The pattern corresponded to anhydrous NiC_2O_4 and NiO (Table 4) [28]. The IR spectrum and X-ray diffraction pattern for the sample decomposed isothermally at 380 °C showed mainly NiO (Table 5); the sample was pale green and had an electrical conductivity value of about $10^{-4}\ \Omega^{-1}\ cm^{-1}$ [29]. The sample thus obtained at 380 °C shows a variation in σ with temperature. This behaviour is characteristic of the non-stoichiometry present in NiO [29,30]. Hence we can infer that the nature of the oxidative decomposition steps for $CoC_2O_4 \cdot 2H_2O$ and $NiC_2O_4 \cdot 2H_2O$ under a static air atmosphere are not generally the same. Thus the conventional simultaneous thermal analysis (TGA and DTA) supplemented with electrical conductivity measurements, IR spectral data,

TABLE 5

X-ray diffraction data for CoO and NiO obtained from $CoC_2O_4 \cdot 2H_2O$ and $NiC_2O_4 \cdot 2H_2O$ by heating in an atmosphere of nitrogen at 380 °C and 400 °C respectively [a]

Observed d spacing for CoO (Å)	Observed d spacing for NiO (Å)
2.48 (70)	2.41 (65)
2.12 (100)	
	2.09 (100)
1.51 (50)	1.47 (30)
1.28 (20)	
1.22 (16)	1.25 (20)
	1.20 (13)
1.06 (10)	1.04 (8)
0.99 (18)	0.96 (5)
0.95 (35)	0.93 (10)
	0.85 (10)

[a] The figures given in parentheses are intensities relative to the linewidth intensity (100).

X-ray diffraction patterns and elemental analyses gave a detailed analysis of the thermal decomposition of $CoC_2O_4 \cdot 2H_2O$ and $NiC_2O_4 \cdot 2H_2O$.

When the reaction is carried out in an atmosphere of static air, the gaseous product acts as a gas buffer for the solid state reaction and some of the reaction is poorly defined. For example, the role of water molecules in $CoC_2O_4 \cdot 2H_2O$ or $NiC_2O_4 \cdot 2H_2O$ and the role of atmospheric oxygen in the solid state reaction in static air could be clarified by comparing the different physical properties for the reaction carried out in a dynamic dry nitrogen atmosphere.

Dynamic nitrogen atmosphere

$CoC_2O_4 \cdot 2H_2O$

The dehydration of $CoC_2O_4 \cdot 2H_2O$ (Fig. 2(a)) was clearly indicated by an endothermic peak in the DTA curve at 230 °C. The TGA curve showed a weight loss within the temperature range 125–270 °C with a plateau up to 350 °C corresponding to the loss of two water molecules. The decomposition of the oxalate (CoC_2O_4) was indicated by an endothermic peak in the DTA curve at 370 °C. The TGA curve showed a continuous weight loss from 350 to 400 °C. This weight loss was found to be in good agreement with the formation of CoO as final product.

The temperature variation of the electrical conductivity σ (Fig. 2(b)) does not show much change with an increase in temperature from 27 to 180 °C (region A). There was a steady increase in the value of σ between 180 and 235 °C (region A′) followed by a linear decrease between 240 and 270 °C

(region B). The isothermally heated sample of $CoC_2O_4 \cdot 2H_2O$ in region A showed no observable change in the IR spectrum and X-ray diffraction pattern (see Table 1). In the temperature range corresponding to region A′ in Fig. 2(b), the IR spectrum showed sharp peaks for the oxalate group frequencies [20,21] and the H–OH band decreased in intensity. The X-ray diffraction pattern also showed broad peaks with no observable change. A sample heated isothermally at 260 °C, (region B of Fig. 2(b)), showed no H–OH band in the IR spectrum. Elemental analysis agreed well with that of the anhydrous compound CoC_2O_4, and the X-ray diffraction pattern indicated a less crystalline sample, with a slight decrease in the interplanar spacings (Table 2). Region B, therefore, corresponded to the dehydration of $CoC_2O_4 \cdot 2H_2O$. After the dehydration step, the value of σ remained constant in the temperature range 270–300 °C. A steep increase in σ from 10^{-9} to 10^{-3} Ω^{-1} cm^{-1} was observed within the temperature range 310–360 °C (region C), and then σ remained constant up to 390 °C (region D). The IR spectrum for a sample heated isothermally in region C showed bands attributed to Co–O stretching frequencies becoming more intense, and a band relating to coordinated carboxylate decreasing in intensity. The X-ray diffraction pattern showed sharp lines, indicating that the sample was predominantly crystalline. The pattern fitted with the data for anhydrous CoC_2O_4 and CoO [23].

The X-ray diffraction pattern of a sample from the dry nitrogen atmosphere run obtained at 390 °C (region D) showed sharp lines and was comparable with the data reported [23] for CoO (Table 5). No line which could be assigned to metallic cobalt could be detected. The sample thus obtained at 390 °C showed a variation in σ with changing temperature. This behaviour is characteristic of CoO [24,25]. The sample was olive green in colour. The Seebeck voltage of this sample under nitrogen atmosphere shows p-type semiconducting properties. Thus the X-ray diffraction patterns and conductivity measurements suggested that the product obtained by thermal decomposition of $CoC_2O_4 \cdot 2H_2O$ in a dry nitrogen atmosphere is pure CoO, and that the concentration of cobalt metal, if present at all, is beyond the detection limit of these techniques.

$NiC_2O_4 \cdot 2H_2O$

The DTA curve in Fig. 2(c) for $NiC_2O_4 \cdot 2H_2O$ showed a broad endothermic peak at 255 °C. The TGA curve showed a weight loss for the dehydration step up to 285 °C corresponding to the loss of two water molecules. However, a peak (B) was found on the plot of log σ against T^{-1}, Fig. 2(d). The IR spectrum of the sample of $NiC_2O_4 \cdot 2H_2O$ isothermally heated at 270 °C showed no H–OH bands. Elemental analysis agreed well with that for the anhydrous compound NiC_2O_4, and the X-ray diffraction pattern indicated that the sample was less crystalline than the starting material

$NiC_2O_4 \cdot 2H_2O$ (Table 1). Region B can therefore be said to correspond to the dehydration of $NiC_2O_4 \cdot 2H_2O$.

A broad endothermic peak on the DTA curve, corresponding to the thermal decomposition occurred at 355 °C. The TGA curve showed a continuous weight loss from 315 °C until it crystallized to mainly NiO. The plot of log σ against T^{-1} was quite similar to that of Fig. 2(b) after the dehydration step. The IR spectrum and X-ray diffraction pattern for a sample heated isothermally in region C showed a mixture of NiC_2O_4 and NiO [2,30]. The X-ray diffraction pattern for a sample from the dry nitrogen atmosphere run obtained at 400 °C (region D) showed sharp lines and was comparable with the data reported [30] for NiO. No line which could be assigned to metallic nickel could be detected. The sample thus obtained in region D shows a variation in σ with a variation in temperature. Thus the X-ray diffraction pattern and conductivity measurements (about 10^{-4} Ω^{-1} cm^{-1}) [28,29] suggested that the product obtained by thermal decomposition of $NiC_2O_4 \cdot 2H_2O$ in a dry nitrogen atmosphere is pure NiO.

Comparison of the solid state thermal decomposition reactions of $CoC_2O_4 \cdot 2H_2O$ and $NiC_2O_4 \cdot 2H_2O$ in normal static air and in dynamic dry nitrogen showed the following main differences.

(a) The temperatures corresponding to dehydration and decomposition from DTA curves recorded under nitrogen atmosphere were resolvable and matched changes observed in plots of log σ vs. T^{-1}, whereas the curves obtained under static air were quite complex.

(b) The decomposition temperatures observed from DTA and TGA curves recorded under a nitrogen atmosphere were higher than those observed under static air.

(c) Oxalate was intimately associated with the decomposition product up to 360 °C in static air and a dry nitrogen atmosphere.

(d) The step corresponding to the formation of anhydrous CoC_2O_4 and NiC_2O_4 was resolved in the plot of log σ vs. T^{-1} for the dry nitrogen atmosphere.

(e) The final products of the decomposition of $CoC_2O_4 \cdot 2H_2O$ and $NiC_2O_4 \cdot 2H_2O$ are Co_3O_4 and NiO in static air, and CoO and NiO in a nitrogen atmosphere respectively.

Because the solid state thermal decomposition of $CoC_2O_4 \cdot 2H_2O$ and $NiC_2O_4 \cdot 2H_2O$ is influenced by the atmosphere, it was decided to undertake similar measurements in other controlled atmospheres.

Dynamic air atmosphere

$CoC_2O_4 \cdot 2H_2O$

The TGA curve showed a weight loss between 120 and 250 °C (Fig. 3(a)). The DTA curve showed an endothermic peak at 210 °C, corresponding to

the dehydration of $CoC_2O_4 \cdot 2H_2O$, and an exothermic peak at 280 °C, corresponding to oxidative decomposition.

Region B in the plots of log σ vs. T^{-1} (Fig. 3(b)) corresponds to the dehydration of $CoC_2O_4 \cdot 2H_2O$. There was a steady increase in σ at 260 °C followed by another steep increase at 325 °C (see regions C and D in Fig. 3(b)). These two temperature ranges, 260–320 °C and 320–390 °C, can be tentatively assigned to the formation of CoO and Co_3O_4, respectively. However, our repeated experiments to obtain pure CoO by careful heating in dynamic air, even at 290 °C, always led to the formation of a mixture of CoO and CoC_2O_4. As the X-ray diffraction pattern of the sample obtained in this way showed broad lines, the product seems to be less crystalline. The IR spectrum of a sample heated isothermally in regions C and D showed broad peaks at 625 and 409 cm^{-1}, which are due to Co–O stretching frequencies [20,21]. Within the temperature range (about 390 °C) of region E in Fig. 3(b), the value of σ remained almost constant. The X-ray diffraction pattern for this region indicated a predominance of Co_3O_4; the sample is black and crystalline.

$NiC_2O_4 \cdot 2H_2O$

The DTA curve in Fig. 3(c) for $NiC_2O_4 \cdot 2H_2O$ showed a broad endothermic peak at 260 °C and the TGA curve indicated a weight loss between 100 and 275 °C, corresponding to the dehydration of $NiC_2O_4 \cdot 2H_2O$. However, a broad peak (B) was found on the plot of log σ vs. T^{-1} (Fig. 3(d)). An exothermic peak on the DTA curve corresponding to the thermal decomposition occurred at 340 °C. The TGA curve showed a continuous weight loss from 310 °C until it crystallized to NiO. The plot of log σ vs. T^{-1} showed a steep increase in σ between 310 and 360 °C (region C) and then remained constant above this temperature (region D). The IR spectra and X-ray diffraction pattern for the sample decomposed isothermally at 400 °C showed mainly NiO; it is a pale green crystalline sample.

The gaseous products obtained by thermal decomposition of $CoC_2O_4 \cdot 2H_2O$ and $NiC_2O_4 \cdot 2H_2O$ under a dynamic (pure and dry) nitrogen atmosphere were indicated by the gas chromatograms (not shown). These chromatograms showed the presence of polar-type gases (namely CO, CO_2, H_2 etc.). The gases were collected at around 380 °C.

The different paths followed by the decomposition of $CoC_2O_4 \cdot 2H_2O$ and $NiC_2O_4 \cdot 2H_2O$ in different atmospheres is now considered. Complete dehydration of $CoC_2O_4 \cdot 2H_2O$ and $NiC_2O_4 \cdot 2H_2O$ was observed under static air, dynamic dry nitrogen and dynamic air atmospheres, as indicated by TGA, DTA and log σ T^{-1} curves. A transformation of CoC_2O_4 to CoO was also detected in static and dynamic air atmospheres. A separate phase of CoO could not be obtained; this compound always occurred with CoC_2O_4. Thus the transformation of CoO and CoC_2O_4 seems to be an equilibrium reaction. This mixture of CoO and CoC_2O_4 is then transformed to Co_3O_4, which is the

final product obtained in static air and dynamic air. These reactions are presented as follows:

$$CoC_2O_4 \cdot 2H_2O \xrightarrow{90\text{–}235\,^\circ C} CoC_2O_4 + 2H_2O\uparrow$$

$$CoC_2O_4 \xrightarrow{235\text{–}290\,^\circ C} CoO + CO\uparrow + CO_2\uparrow$$

$$2CoO + CoC_2O_4 \xrightarrow{290\text{–}400\,^\circ C} Co_3O_4 + 2CO\uparrow$$

The transformation of CoC_2O_4 to CoO was the final step detected in a dynamic dry nitrogen atmosphere, while NiC_2O_4 transformed to NiO under static air, dynamic dry nitrogen and dynamic air atmospheres:

$$NiC_2O_4 \cdot 2H_2O \xrightarrow{90\text{–}280\,^\circ C} NiC_2O_4 + 2H_2O\uparrow$$

$$2NiC_2O_4 \xrightarrow{280\text{–}360\,^\circ C} NiC_2O_4 + NiO + CO\uparrow + CO_2\uparrow$$

$$NiC_2O_4 + NiO \xrightarrow{360\text{–}400\,^\circ C} 2NiO + CO\uparrow + CO_2\uparrow$$

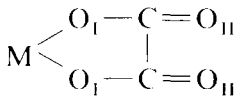

Scheme 1

It has been reported in the literature [5] that as the M–O_I bond (Scheme 1) becomes stronger, so the C–O_I bond is lengthened and the C–O_{II} bond is shortened. As the electronegativity of the metal ion increases so the bond strength of the M–O_I bond will increase and according to Fujita et al. [31] the C–O_I bond will become weaker. This also depends on whether the standard free energy of formation ($\Delta G^\ominus$) of the oxide MO from its elements is greater or less than $\Delta G^\ominus$ for the formation of CO_2 from 2CO and O_2 [2]. In the present study, the final products, cobalt oxide or nickel oxide, were produced in a nitrogen atmosphere. The decomposition temperature represents the energy required to break the C–O_I bond, and this will depend less critically on the nature of the cation.

CONCLUSIONS

The results of the present study allow us to make the following important observations regarding the solid state decompositions of $CoC_2O_4 \cdot 2H_2O$ and $NiC_2O_4 \cdot 2H_2O$.

(a) The dehydration of $CoC_2O_4 \cdot 2H_2O$ and $NiC_2O_4 \cdot 2H_2O$, yielding anhydrous CoC_2O_4 or NiC_2O_4, took place in all three of the atmospheres considered.

(b) Conventional thermal analysis curves (TGA, DTA) showed a very broad large exothermic peak (DTA) and continuous weight loss (TGA) for

the oxalate in all three atmospheres during the oxidative decomposition step. These curves could not, however, provide information regarding the type of intermediates formed at this step. Hence, it was necessary to supplement the results with a more helpful technique, i.e. the use of d.c. electrical conductivity measurements, in conjuction with IR spectral and X-ray diffraction investigations.

(c) In dry nitrogen, the plot of log σ vs. T^{-1} showed a well-characterized step corresponding to dehydration. The formation of CoO from $CoC_2O_4 \cdot 2H_2O$ was confirmed in dry nitrogen atmosphere.

(d) The final product of decomposition in static air and dynamic air was found to be Co_3O_4 for $CoC_2O_4 \cdot 2H_2O$. However, the final decomposition product in all three atmospheres was found to be NiO for $NiC_2O_4 \cdot 2H_2O$.

(e) Gas chromatograms showed that polar gases were present during the thermal decomposition of $CoC_2O_4 \cdot 2H_2O$ or $NiC_2O_4 \cdot 2H_2O$.

ACKNOWLEDGEMENT

The authors are grateful to the Head, Department of Chemistry, University of Poona, Pune 411 007, for his interest and encouragement.

REFERENCES

1 E.D. Macklen, J. Inorg. Nucl. Chem., 29 (1967) 1229.
2 J. Robin, Bull. Soc. Chim. Fr., (1953) 1078.
3 K. Kawagaki, J. Chem. Soc. Jpn., 72 (1951) 1079.
4 R. David, Bull. Soc. Chim. Fr., (1960) 719.
5 D. Dollimore, D.L. Griffiths and D. Nicholson, J. Chem. Soc., (1963) 2617.
6 C. Duval, Inorganic Thermogravimetric Analysis, Elsevier, Amsterdam, 1963.
7 H.G. Wiedeman and D. Nehring, Z. Anorg. Allg. Chem., 304 (1960) 137.
8 J.L. Doremieux and A. Boulle, C.R. Acad. Sci., 250 (1960) 3184.
9 Ya. A. Ugai, Zh. Obsch. Khim., 24 (1954) 1315.
10 J. Amiel and C. Paulmier, C.R. Acad. Sci., 255 (1962) 2443.
11 P.D. Garn and J.E. Kessler, Anal. Chem., 32 (1960) 1565.
12 K.S. Rane, A.K. Nikumbh and A.J. Mukhedkar, J. Mater. Sci., 16 (1981) 2387.
13 A. Venkataraman, V.A. Mukhedkar, M.M. Rahman, A.K . Nikumbh and A.J. Mukhedkar, Thermochim. Acta, 112 (1987) 231.
14 A. Venkataraman, V.A. Mukhedkar, M.M. Rahman, A.K. Nikumbh and A.J. Mukhedkar, Thermochim. Acta, 115 (1987) 215.
15 M.M. Rahman, V.A. Mukhedkar, A. Venkataraman, A.K. Nikumbh, S.B. Kulkarni and A.J. Mukhedkar, Thermochim. Acta, 125 (1988) 173.
16 A.K. Nikumbh, M.M. Rahman and A.D. Aware, Thermochim. Acta, 159 (1990) 109.
17 D. Dollimore and D. Nicholson, J. Chem. Soc., (1962) 960.
18 ASTM File, No. 25–251.
19 ASTM File, No. 25–581.
20 J. Fujita, A.E. Martell and K. Nakamoto, J. Chem. Phys., 36 (1962) 324.
21 J. Fujita, A.E. Martell and K. Nakamoto, J. Chem. Phys., 36 (1962) 331.
22 A.K. Nikumbh, K.S. Rane and A.J. Mukhedkar, J. Mater. Sci., 17 (1982) 2503.
23 ASTM File, No. 9-402.

24 W. Mayer, Z. Elektrochem., 50 (1944) 274.
25 D.J. Craik, Magnetic Oxides, Vol. 1, Wiley Interscience, New York, 1975 p. 450.
26 ASTM File, No. 9–418.
27 B.T. Kolomiets, I.T. Sheftel and E.V. Kurlina, Zh. Tekh. Fiz., 27 (1) (1957) 51.
28 ASTM File, No. 22–1189.
29 W.D. Kingery, Introduction to Ceramics, Wiley, New York, 1960.
30 S.P. Mitoff, J. Chem. Phys., 35 (3) (1961) 882.
31 J. Fujita, K. Nakamoto and M. Kobayashi, J. Phys. Chem., 61 (1957) 1014.